Oscillations of atomic fermions in a one-dimensional optical lattice

T. A. B. Kennedy
Dipartimento di Fisica e Matematica, Università dell'Insubria, via Valleggio 11, 22100 Como, Italy
and School of Physics, Georgia Institute of Technology, Atlanta, Georgia 30332-0430, USA
(Received 5 February 2004; published 12 August 2004)

A semiclassical model is used to investigate oscillations of atomic fermions in a combined magnetic trap and one-dimensional optical lattice potential following axial displacement of the trap. The oscillations are shown to be strongly suppressed on the scale of the displacement, and to have a characteristic small amplitude, damped behavior in the collisionless regime. The presence of a separatrix in the semiclassical Brillouin-zone phase space is predicted and shown to produce strongly asymmetric phase-space distributions as a function of the trap displacement.

DOI: 10.1103/PhysRevA.70.023603 PACS number(s): 03.75.Ss, 05.30.Fk

I. INTRODUCTION

The recent advances in the cooling of atomic Bose and Fermi gases to degeneracy, and the simplicity with which the gas can be confined in a periodic optical lattice potential provide a new point of departure for quantum transport studies of atomic bosons [1–5] and fermions [6–9]. In particular, neutral atomic fermions form a nearly ideal gas at nanokelvin temperatures, and by contrast to conduction electrons in solids, can traverse the dimensions of the Brillouin zone without collision. An ultracold atomic gas is also typically inhomogeneous as a result of magnetic or optical trapping, so that even single particle dynamics can dramatically alter the spatial density distribution of the atomic cloud in an optical lattice.

In a recent experiment a gas of fermionic ^{40}K atoms was evaporatively cooled in a combined magnetic and optical lattice potential, leading to a degenerate cloud at a temperature of a fraction of the Fermi temperature T_F, approximately $0.3T_F$, for the cloud of atoms [9]. Specifically, the experiment involved a configuration with a one-dimensional axial lattice potential produced by a standing wave laser field, with tight magnetic confinement in the transverse plane, but a weaker magnetic trap in the direction coaxial with the lattice thereby emphasizing the latter's role. By displacing the center of the axial magnetic field with respect to the lattice, dipolar oscillations of the Fermi cloud in the lattice potential were investigated. While one might naively expect the resulting motion of the cloud to be comparable to the trap displacement, the principal observations were that the amplitude of the oscillations was significantly smaller than the trap displacement, and it was damped over several periods of the motion.

In this paper we show that these observations can be explained by a simple semiclassical theory of collisionless atomic fermion motion in the combined magneto-optical potential. This confirms the qualitative physical picture discussed in Ref. [9]. The effects of fermion statistics are felt only in the initial conditions. Since the periodic lattice potential is present in the axial direction, it is appropriate to refer to the particle quasimomentum associated with the discrete translational invariance, rather than to the kinetic momentum; quasimomentum is conserved by the lattice forces and changes only due to external forces. By a process of evaporative cooling, a broad distribution of occupied axial quasimomentum states is created, in which the atoms undergo radial harmonic motion. The distribution is necessarily broad on account of the Pauli exclusion principle which excludes two fermions from occupying the same single particle state. In a semiclassical picture the lattice transport dynamics can in principle be determined by following the particle trajectories in a Brillouin-zone phase space consisting of atomic position and quasimomentum. In the Fermi transport problem we study here, we are able to do this explicitly in the reduced two-dimensional phase space in which the single particle states are labelled by the axial components of position and quasimomentum. The atoms meanwhile also perform radial harmonic motion in orbits whose amplitudes are governed by the initial temperature of the cloud. However, since the radial and axial motion are uncoupled, the effects of radial motion on the axial distribution function is easily accounted for.

The remainder of the paper is organized as follows. In Sec. II we develop a theoretical model for the dynamics of the degenerate cloud in the confined magnetic and optical lattice potentials. In Sec. III we discuss the semiclassical distribution function on the axial Brillouin-zone phase space, and illustrate how the trap displacement influences the evolution of the distribution function, and the center of mass motion of the cloud. Finally, in Sec. IV we summarize our conclusions.

II. SEMICLASSICAL ATOMIC PHASE-SPACE TRAJECTORIES

The Hamiltonian for single particle motion in a combined optical lattice and magnetic confining potential may be usefully written in the following form:

$$H = H_0 + H_1 + V(z), \tag{1}$$

where $H_0 = (p_x^2 + p_y^2)/(2m) + m\omega_r^2(x^2+y^2)/2$, $H_1 = p_z^2/2m + V_0 \sin^2 k_L z$ and $V(z) = m\omega_a^2 z^2/2$. The Hamiltonian H_0 governs the radial harmonic motion produced by the magnetic trap, while $V(z)$ is the residual part of the magnetic confine-

ment in the axial direction. For tight radial confinement $\omega_r \gg \omega_a$. The Hamiltonian $H_1(z)=H_1(z+a)$ describes one-dimensional motion in an optical lattice with period $a=\lambda_L/2$, where λ_L is the optical wavelength and $k_L=2\pi/\lambda_L$ is the wave number. The lattice depth $V_0=sE_r$ is conventionally parametrized by a dimensionless multiple s, of the atomic recoil energy $E_r=\hbar^2k_L^2/(2m)$.

We are here interested in the following specific experimental situation. A single component Fermi gas is cooled to degeneracy in the combined magnetic and optical lattice potential to well below the Fermi temperature T_F. The axial potential is then rapidly displaced $V(z)\rightarrow V(z-d)$, and the degenerate gas performs oscillations in the lattice. These oscillations were observed by waiting for some time before switching off both magnetic and trap potentials and imaging the cloud after a period of ballistic expansion [9].

The one-dimensional lattice Hamiltonian H_1 has Bloch eigenfunctions $\psi_{\alpha q}(z)$ and eigenvalues $\mathcal{E}_\alpha(q)=\mathcal{E}_\alpha(q+K)$ with $K=(2\pi/a)\times$(integer), any reciprocal-lattice vector. Here $\hbar q$ is the axial quasimomentum associated with translations $z\rightarrow z+a$ in the periodic lattice, and α is the integer axial band index. We employ a semiclassical approach to treat the transport dynamics of the atomic fermions in the axial direction. The method is well suited to the description of the collisionless regime relevant to single component ultracold fermions where s-wave scattering is prohibited by the antisymmetry of the two-body wave function and p-wave scattering is strongly suppressed. The energy bands implicitly take into account the axial lattice potential responsible for large changes in the physical momentum of the moving particle, but which conserve the quasimomentum $\hbar q$. We assume, consistent with Ref. [9], that only the fundamental axial band $\alpha=1$ is populated at the temperatures of interest, and therefore we will suppress the axial band index. The effects of radial quantum mechanical motion, which results in a set of harmonic orbits labelled by the radial quantum number $n_r=0,1,\ldots$, will be taken into account in the following section when we discuss the axial phase-space distribution function.

In the semiclassical theory, motion of an atom is considered to be restricted to a given energy band, and only external forces other than the lattice, in this case due to the magnetic trap, can change its quasimomentum. It follows that the axial motion of a fiducial atom, in response to the axial displacement d of the trap, is found by solving the equations of motion (for $t\geqslant 0$)

$$\hbar\dot{q}(t) = -m\omega_a^2[z(t)-d],$$

$$\dot{z}(t) = \frac{1}{\hbar}\frac{\partial\mathcal{E}(q)}{\partial q}. \tag{2}$$

We note that these equations are independent of the motion in the transverse xy plane.

As a simple example consider motion confined to near the bottom of the fundamental axial band, but with arbitrary radial excitation. We may write $\mathcal{E}(q)=\hbar^2q^2/(2m_{\rm eff})+$constant, with $m_{\rm eff}$ the associated effective mass. The equations of motion reduce to

$$\frac{d^2z(t)}{dt^2} = -\Omega^2[z(t)-d], \tag{3}$$

describing harmonic oscillations about the displaced position d with renormalized frequency $\Omega=\sqrt{m/m_{\rm eff}}\omega_a$ [10]. The harmonic approximation predicts large amplitude dipole oscillations but cannot correctly describe the orbits of occupied fermionic states with relatively large axial quasimomentum far from the band minimum. On the other hand, a Bose condensate would have a narrow quasimomentum distribution [4]. The simple harmonic theory indicates that one should expect large amplitude dipole oscillations in this case, as has been observed in experiments [9,11]. An ideal gas model with a narrow quasimomentum distribution is, however, not sufficient to correctly describe superfluid effects associated with an interacting Bose condensate [12].

It therefore appears that nonharmonic orbits are the key to explaining the experimental observations of suppressed dipole oscillations. In order to analyze such orbits we note that any axial energy band must satisfy the periodicity requirement $\mathcal{E}(q)=\mathcal{E}(q+K)$. For example, the axial energy band

$$\mathcal{E}(q) = e_0\sin^2\left(\frac{\pi q}{2k_L}\right), \tag{4}$$

with the band depth $e_0=(4m/\pi^2m_{\rm eff})E_r\sim 0.4(m/m_{\rm eff})E_r$, behaves like $\hbar^2q^2/(2m_{\rm eff})$ for small q, but also satisfies the periodicity requirement with period $2k_L$. Thus all physically distinct states of a single fermionic atom lie in the range $-k_L<q\leqslant k_L$. The shape of this model band is qualitatively similar to that of the true lattice potential $sE_r\sin^2 k_Lz$. In Ref. [9], results for $s=8$, a relatively deep lattice are presented. For larger values of s tunneling becomes increasingly suppressed, and it is in the same limit that the form Eq. (4) may be derived in a tight binding approximation. For ^{40}K in the true lattice potential, the fundamental band depth varies monotonically between $0.77E_r$ for $s=1$ and $0.12E_r$ for $s=8$, the largest value achieved in Ref. [9]. Were it necessary, we could choose the value of $m_{\rm eff}$ in the model band to agree with the true band depth. However, our goal here is not a quantitative analysis of the experiments, but a qualitative explanation of the results. The latter, depends on the existence of harmonic and nonharmonic orbits and phase-space structures which are more easily demonstrated by using the model energy band. It has the advantage over the true energy band, of enabling analytic calculation of all the atomic orbits in terms of physical pendulum dynamics, and moreover, this greatly facilitates the calculation of the phase-space distribution function in the following section. For the model of Eq. (4) the equations of motion are

$$\hbar\dot{q}(t) = -m\omega_a^2[z(t)-d], \tag{5}$$

$$\dot{z}(t) = \frac{\hbar k_L}{m_{\rm eff}\,\pi}\sin\left(\frac{\pi q(t)}{k_L}\right). \tag{6}$$

Eliminating z and defining the dimensionless quasimomentum $Q\equiv\pi q/(2k_L)$ we get the conservation equation

$$\frac{d}{dt}[\dot{Q}(t)^2 + \Omega^2 \sin^2 Q(t)] = 0. \tag{7}$$

The first integral may be written $\dot{Q}(t)^2 + \Omega^2 \sin^2 Q(t) = \Omega^2 M$ where M is fixed for a given orbit. Physically M measures the conserved "energy" of the fictitious pendulum orbit in units of the fundamental band depth e_0. Details of the corresponding orbits are given in the Appendix.

The value of M depends on the trap displacement and satisfies the "energy" conservation condition,

$$[z(t) - d]^2 + \ell^2 \sin^2 Q(t) = \ell^2 M, \tag{8}$$

where we define the length scale

$$\ell = \frac{2}{\pi}\sqrt{\frac{2E_r}{m_{\rm eff}\,\omega_a^2}}, \tag{9}$$

such that the band depth $e_0 = m\omega_a^2 \ell^2/2$. For $M \leqslant 1$, the orbits in the $z-q$ phase space are closed, whereas for $M > 1$ they are open. The separatrix orbit $M=1$ has homoclinic fixed points on the Brillouin-zone boundary, analogous to the infinite period motion of a physical pendulum between vertically upwards initial and final positions, $\sin Q(t) = \tanh(\pm\Omega t + \phi_1)$ and $[z(t)-d]/\ell = \mp \mathrm{sech}(\pm\Omega t + \phi_1)$. The qualitatively different character of these orbits is responsible for a nontrivial dependence of the dipole oscillations on the trap displacement d. When the trap is displaced $z \to z-d$, the peak of the phase-space distribution function remains at $z=0$, but the separatrix is given by Eq. (8) with $M=1$, and is centered in the region $z>0$. Subsequently the atoms lying inside the separatrix will perform closed orbits, while those left outside remain outside, and perform small amplitude spatial oscillations as they traverse the Brillouin zone. The relative importance of the two sets of orbits in the overall motion of the cloud is determined by the fraction of atoms initially inside and outside the separatrix. In turn, this is governed by the magnitude of the initial displacement d relative to ℓ. As we will illustrate in the following section, the axial distribution function can develop strong asymmetry for large trap displacements, due to the separatrix structure of the Brillouin-zone phase space.

III. DYNAMICS OF THE AXIAL ATOMIC DISTRIBUTION FUNCTION

The initial thermal distribution of atomic fermions produced by evaporative cooling in the combined magnetic trap and optical lattice potentials, can be written in terms of a semiclassical distribution function for motion in the axial direction with the radial harmonic oscillator quantum numbers n_x and n_y. Since the radial potential is assumed to be azimuthally symmetric, only the combination $n_r = n_x + n_y$ arises. Recall that we assume the temperature is sufficiently low that only the lowest axial band is populated [9]. We are therefore left to consider a set of axial distribution functions with different radial quantum numbers. Specifically, the initial axial distribution function is given by $f^{(0)}(z,q) = \sum_{n_r=0}^{\infty} f_{n_r}^{(0)}(z,q)$, where

$$f_{n_r}^{(0)}(z,q) = (n_r+1)[e^{\beta(n_r\hbar\omega_r + \mathcal{E}(q) + V(z) - \mu)} + 1]^{-1}, \tag{10}$$

with $\beta = 1/(k_B T)$, $n_r = 0,1,2,\ldots$ the radial quantum number and μ the chemical potential. Note that, due to the lattice, this is a function of z and quasimomentum $\hbar q$, as opposed to physical momentum. The factor (n_r+1) is the degeneracy of the radial band with energy $\hbar\omega_r n_r$ above the ground state $n_r = 0$. The distribution function is assumed not to change if the axial trap is displaced rapidly. The subsequent collisionless motion of the cloud causes the distribution to change according to the Boltzmann equation

$$\frac{\partial f_{n_r}}{\partial t} + \frac{\partial \mathcal{E}(q)}{\partial \hbar q}\frac{\partial f_{n_r}}{\partial z} - m\omega_a^2 (z-d)\frac{\partial f_{n_r}}{\partial q} = 0, \tag{11}$$

with solution

$$f_{n_r}(z(t), q(t)) = f_{n_r}^{(0)}(z(0), q(0)). \tag{12}$$

Using the analysis in the Appendix we have that, for bound orbits $M < 1$,

$$\sin Q(t) = \frac{\sin Q(0)\mathrm{cn}(\Omega t)\mathrm{dn}(\Omega t) - \dfrac{[z(0)-d]}{\ell}\cos Q(0)\mathrm{sn}(\Omega t)}{1 - \sin^2 Q(0)\mathrm{sn}^2(\Omega t)},$$

$$z(t) - d = \frac{[z(0)-d]\mathrm{cn}(\Omega t) + \ell \sin Q(0)\cos Q(0)\mathrm{sn}(\Omega t)\mathrm{dn}(\Omega t)}{1 - \sin^2 Q(0)\mathrm{sn}^2(\Omega t)}, \tag{13}$$

where we note that $\mathrm{dn}(\phi_M | M) = \cos Q(0) \geqslant 0$ in the first Brillouin zone, and $\mathrm{sn}(\Omega t) \equiv \mathrm{sn}(\Omega t | M)$; similarly for cn and dn. For the open orbits $M > 1$, the following expressions hold

$$\sin Q(t) = \frac{\sin Q(0)\mathrm{cn}(\omega t)\mathrm{dn}(\omega t) - \dfrac{[z(0)-d]}{\ell\sqrt{M}}\cos Q(0)\mathrm{sn}(\omega t)}{1 - \sin^2 Q(0)\mathrm{sn}^2(\omega t)/M},$$

$$z(t) - d = \frac{[z(0)-d]\mathrm{dn}(\omega t) + \dfrac{\ell}{\sqrt{M}}\sin Q(0)\cos Q(0)\mathrm{sn}(\omega t)\mathrm{cn}(\omega t)}{1 - \sin^2 Q(0)\mathrm{sn}^2(\omega t)/M}, \tag{14}$$

where we note $\mathrm{cn}(\phi_{1/M} | 1/M) = \cos Q(0)$ and $\mathrm{sn}(\omega t) \equiv \mathrm{sn}(\sqrt{M}\Omega t | 1/M)$, etc.

The axial number density of fermions in radial band n_r at time t, is given by integrating over the quasimomentum of a single Brillouin zone,

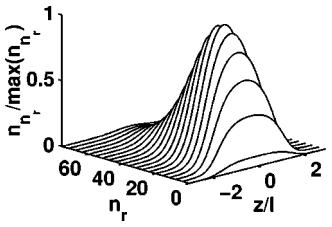

FIG. 1. The initial atomic density, scaled to its maximum value over the range, is shown as a function of the radial quantum number n_r. The total axial density $n(z,0)$ is found by summation over n_r. Parameters are given in the body of the text.

$$n_{n_r}(z,t) = \int_{-k_L}^{k_L} \frac{dq}{2\pi} f_{n_r}(z,q,t), \tag{15}$$

and the total axial column density $n(z,t)=\Sigma_{n_r=0}^{\infty} n_{n_r}(z,t)$. Similarly, the distribution of quasimomentum can be computed by summation of the distribution functions for the individual radial energy bands, $n_{n_r}(q,t)=\int dz\, f_{n_r}(z,q,t)$.

In Fig. 1 we show the initial spatial density as a function of radial quantum number n_r and z at a temperature $T \approx 0.3T_F$. We have taken the experimental parameters from Ref. [9], except that we use the analytical model energy band of Eq. (4), rather than the numerical result appropriate to the optical standing wave. We emphasize that the results presented are not intended for quantitative comparison with the results of the experiment in Ref. [9]. However, since the qualitative features of the model energy band are the same as those shown in Ref. [9], its predictions should be in qualitative agreement. The parameters employed in the figures are given here mainly in units of temperature, therefore energies are recovered by multiplying by Boltzmann's constant. We consider ^{40}K atoms cooled in a magnetic trap with radial and axial frequencies $\omega_r=15.2$ nK and $\omega_a=1.15$ nK, respectively. The wavelength of the incident light is taken to be $\lambda_L=754$ nm. The chemical potential $\mu=430$ nK, and $\beta=6.98$ $(\mathrm{MK})^{-1}$. For our model axial energy band, assuming $m_{\mathrm{eff}}=m$ for simplicity, this gives the length scale $\ell \approx 55.5$ μm and band depth $e_0 \approx 170$ nK. A density plot of the initial distribution function is shown in Fig. 2, along with the separatrix trajectory in the phase space following trap displacement $(M=1)$. Orbits inside and outside the separatrix follow its contour precisely as occurs in the case of the mechanical pendulum. In this example we assume a trap displacement $d=15$ μm much less than ℓ, so that the bulk of the atomic distribution lies inside the separatrix, and therefore most though not all particles will undergo bound orbits in the first Brillouin zone.

The dynamics of the particle distribution in each radial band can be calculated separately, as explained above, and then summed over the radial quantum number n_r to get the total axial distribution function. However, the latter summation is unnecessary for a qualitative understanding of the dynamics. Each radial band distribution function has the same dynamics, because the phase-space trajectories $\mathbf{(}z(t),q(t)\mathbf{)}$ are independent of the radial quantum number n_r. In particular the damped motion of the cloud center of mass

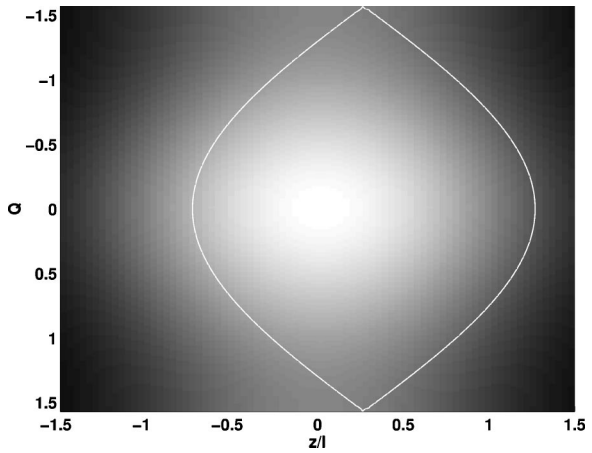

FIG. 2. The initial axial atomic distribution function in the z-Q phase space for $d=15$ μm. The oval shaped contour is the separatrix across which particles may not cross during the collisionless dynamics. Other parameters are the same as in Fig. 1.

is evident in the distribution function $f_{n_r}(z,q,t)$ dynamics, for a fixed radial quantum number n_r. In Fig. 3 we show the total axial distribution which evolves from the initial distribution shown in Fig. 2 at time $\Omega t_f=15$. During this time, the center of mass of each radial band density undergoes a similar damped dipole oscillation leading to the center of mass dynamics for the cloud illustrated in Fig. 4. We note that the amplitude of the oscillation is small compared to the displacement of the trap center, in qualitative agreement with the observations of Ref. [9]. The damping is caused by the stretching of the distribution function along the phase-space trajectories, not by collisions, dissipation or the influence of different radial orbits. It is straightforward to check, and is indeed obvious in the limit of a very narrow distribution in (z,Q) phase space, that the damping is correspondingly reduced. However, a Fermi distribution must necessarily have a broad distribution of Q states on account of the Pauli exclusion principle. Damping is therefore a feature of collisionless Fermi transport dynamics. A narrow quasimomentum

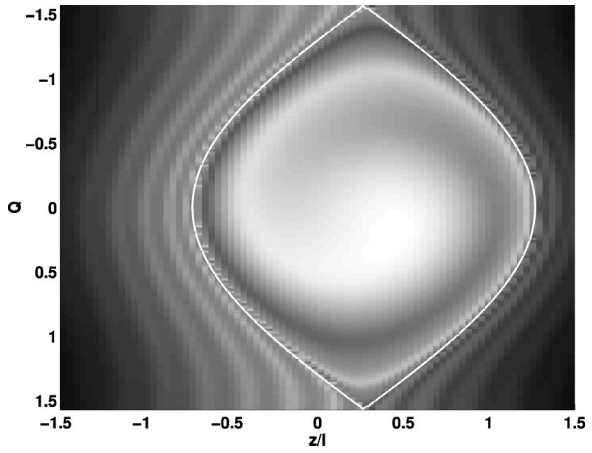

FIG. 3. The axial atomic distribution function at $\Omega t=15$, in the z-Q phase space for $d=15$ μm. The region of high density lies inside the separatrix, but has been stretched out over the region. Other parameters are the same as in Fig. 1.

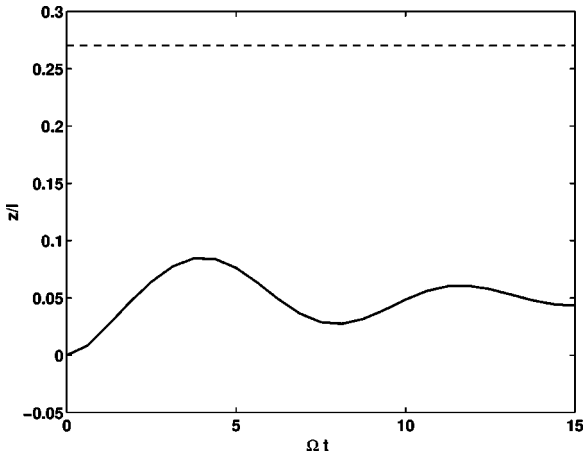

FIG. 4. Small amplitude damped oscillation of the axial component of the cloud center of mass near the undisplaced center of the cloud $z=0$. The position of the displaced trap center is shown by the dashed line. Other parameters are the same as in Fig. 1.

distribution is predicted also by the Gross-Pitaevski dynamics of a superfluid Bose condensate in a lattice, and in this case undamped oscillations have been observed [9,11].

The nonharmonic orbits of large axial quasimomentum which are necessarily populated in a Fermi gas cause the stretching of the distribution function both inside and outside the separatrix. As noted above, each radial band executes a similar damped motion in phase with the others. In Figs. 5 and 6 we illustrate the dynamics of the axial distribution function for a larger trap displacement $d=45$ μm, a value which is comparable to the separatrix distance $\ell \approx 55$ μm. In this case a fraction approaching one-half of the particles now follow open orbits in the first Brillouin zone. The total distribution function develops strong whorls inside the separatrix and spatial oscillations occur in the exterior. The Brillouin-zone periodicity implies particle trajectories which enter or exit at $Q=\pi/2$, exit or enter at $Q=-\pi/2$. The basic left-right asymmetry survives the integration over the quasimomentum required to determine the axial spatial density,

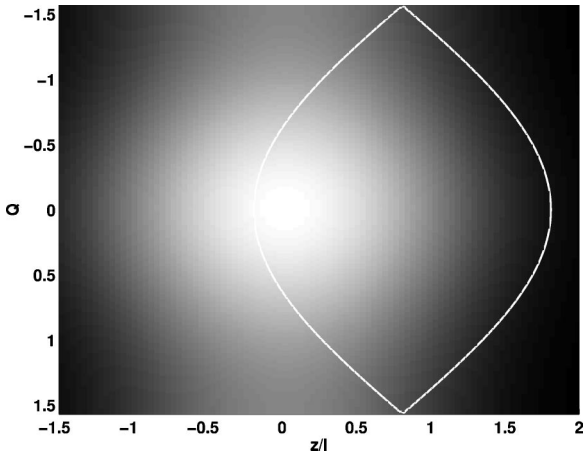

FIG. 5. The initial atomic distribution function in the z-Q phase space for $d=45$ μm. The region of high density traverses the phase-space separatrix. Other parameters are the same as in Fig. 1.

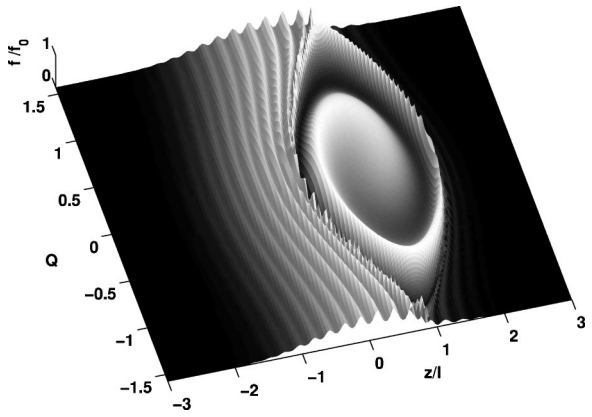

FIG. 6. The atomic distribution function, scaled to its maximum value over the range f_0, is shown on the z-Q phase space at $\Omega t_f = 15$ for $d=45$ μm. The complicated structure reflects the open and closed orbits in the first Brillouin zone, which lead to a strong asymmetry. Other parameters are the same as in Fig. 1.

but the center of mass motion is qualitatively similar to that illustrated in Fig. 4. Interestingly, for a broad distribution of Q values, both closed and open orbits produce small amplitude center of mass oscillations. The presence of the separatrix structure could be investigated experimentally if the amplitude of center of mass oscillations were systematically studied as a function of trap displacement d. Alternatively, direct measurements of the axial spatial density or the phase-space distribution function would be particularly interesting.

IV. CONCLUSION

We have shown that a simple semiclassical theory of the axial motion of a gas of atomic fermions, without any collisional interactions, produces transport dynamics in qualitative agreement with recent experimental observations [9]. The gas executes damped oscillations with an amplitude small compared to the axial magnetic trap displacement. We also point out the presence of a separatrix in the Brillouin-zone phase space which produces strong asymmetries in the axial phase space distribution and axial density functions. It would be interesting to investigate this structure further experimentally, for example, by looking for nonmonotonic behavior of the transport properties as a function of the initial trap displacement d.

ACKNOWLEDGMENTS

The authors thank M. Inguscio and G. Roati for interactions which led to the present work and S. D. Jenkins for discussions. We also acknowledge the support of MIUR and the hospitality of the Università dell'Insubria where this work was carried out.

APPENDIX: PHASE-SPACE ORBITS

In this appendix, we present the analytical details of the pendulum dynamics used in constructing the dynamics of the semiclassical fermionic phase-space distribution function. It

is useful to present these for $M>1$ and $M<1$ separately, as the form of the orbits is qualitatively different in the two cases, corresponding to rotating and bound orbits, respectively, of a physical pendulum. The solution of Eq. (7) is given by

$$\sin Q(t) = \sqrt{M}\,\mathrm{sn}(\pm\Omega t + \phi_M|M), \tag{A1}$$

where the initial phase

$$\phi_M = u(\sin Q(0)/\sqrt{M}|M) \tag{A2}$$

is given in terms of the Legendre elliptic function of the first kind $u(x|m)$. Using the identities

$$\mathrm{sn}(x|M) = \mathrm{sn}(\sqrt{M}x|1/M)/\sqrt{M}$$

and

$$\sqrt{M}u(\sin\phi|M) = u(\sqrt{M}\sin\phi|1/M),$$

we can also write

$$\sin Q(t) = \mathrm{sn}(\pm\sqrt{M}\Omega t + \phi_{1/M}|1/M), \tag{A3}$$

where the initial phase $\phi_{1/M}=\phi_M\sqrt{M}$ is given by

$$\phi_{1/M} = u(\sin Q(0)|1/M). \tag{A4}$$

We present these results in terms of elliptic functions in which the amplitude argument, either M or $1/M$, is in the range [0,1]. This is useful for the comparison of orbits with $M<1$ and $1/M<1$. These orbits are analogous to the oscillating and rotating orbits, respectively, of a mechanical pendulum.

Differentiation of the result for $\sin Q(t)$ with respect to time yields

$$\dot{Q}(t) = \pm\Omega\sqrt{M}\,\mathrm{cn}(\pm\Omega t + \phi_M|M), \tag{A5}$$

which in turn gives the atomic trajectories

$$z(t) - d = \mp\ell\sqrt{M}\,\mathrm{cn}(\pm\Omega t + \phi_M|M) \tag{A6}$$

or, using $\mathrm{cn}(x|M)\equiv\mathrm{dn}(\sqrt{M}x|1/M)$,

$$z(t) - d = \mp\ell\sqrt{M}\,\mathrm{dn}(\pm\sqrt{M}\Omega t + \phi_{1/M}|1/M).$$

Expanding these results using double angle formulas for the Jacobian elliptic functions one readily derives Eqs. (13) and (14).

[1] F. S. Cataliotti, S. Burger, C. Fort, P. Maddaloni, F. Minardi, A. Trombettoni, A. Smerzi, and M. Inguscio, Science **293**, 843 (2001).

[2] B. P. Anderson and M. A. Kasevich, Science **281**, 1686 (2001).

[3] O. Morsch, J. H. Müller, M. Cristiani, D. Ciampini, and E. Arimondo, Phys. Rev. Lett. **87**, 140402 (2001).

[4] J. H. Denschlag, J. E. Simsarian, H. Häffner, C. McKenzie, A. Browaeys, D. Cho, K. Helmerson, S. L. Rolston, and W. D. Phillips, J. Phys. B **35**, 3095 (2002).

[5] M. Greiner, O. Mandel, T. Esslinger, and T. W. Hänsch, Nature (London) **415**, 39 (2002).

[6] W. Hofstetter, J. I. Cirac, P. Zoller, E. Demler, and M. D. Lukin, Phys. Rev. Lett. **89**, 220407 (2002).

[7] M. Rodrigues and P. Törma, e-print cond-mat/0303634.

[8] A. Albus, F. Illuminati, and J. Eisert, e-print cond-mat/0304223.

[9] G. Modugno, F. Ferlaino, R. Heidemann, G. Roati, and M. Inguscio, Phys. Rev. A **68**, 011601(R) (2003).

[10] J. Javanainen, Phys. Rev. A **60**, 4902 (1999).

[11] S. Burger, F. S. Cataliotti, C. Fort, F. Minardi, and M. Inguscio, Phys. Rev. Lett. **86**, 4447 (2001).

[12] M. Krämer, L. P. Pitaevskii, and S. Stringari, Phys. Rev. Lett. **88**, 180404 (2002).